Imperial College London

MSc Applied Mathematics Project

Imperial College London

Department of Mathematics

Advanced Numerical Algorithms for the Simulation of Weather Fronts

Author:
Chloe Raymont

CID:
00733439

Supervisor:
Dr. Colin Cotter

Second Marker:

August 23, 2018

Abstract

Your abstract goes here

Acknowledgements

Declaration

The work contained in this thesis is my own work unless otherwise stated

Contents

List of Figures

Chapter 1

Introduction

Chapter 2

The Governing Equations

The semi-geostrophic equations first introduced by [1] form the basis of our model for frontogenesis. Widely noted to be more rigorous than the classical quasi-geostrophic equations in their description of the formation of weather fronts [2, 3]. In this chapter a summary of key steps that lead to the Eady model for frontogensis that was developed by Hoskins and Bretherton , 1972, [4] is given. Based on the model for baroclinic instability proposed by Eady, 1949, incorporating a linear stratification in density and a constant vertical shear in the horizontal velocity component. A co-ordinate transform to geostrophic co-ordinates by [3] facilitates the numerical implementation of these equations and subsequent interpretation of results. For the following the main points are summarised from Cullen 2006 [2] in formulating the model to be implemented numerically.

2.1 The Semi-Geostrophic Equations

2.1.1 The 3D Incompressible Boussinesq Equations

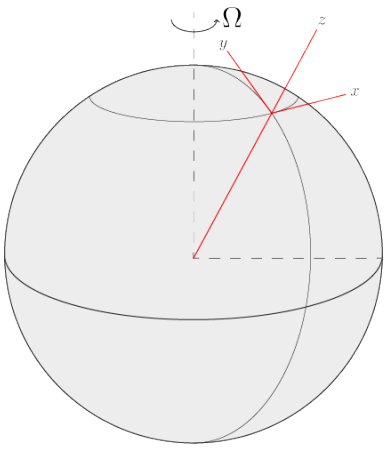

Figure 2.1: Local cartesian co-ordinates (x, y, z) on Earth

We begin with the 3D incompressible Boussinesq equations 2.1 to describe atmospheric flow. Adopting cartesian co-ordinates (x, y, z) representing the zonal, meridional and radial directions on the Earth respectively, as shown in 2.1. The corresponding velocity components are $\boldsymbol{u} = (u, v, w)$, with ρ_0 representing the constant density and p denoting the pressure.

$$\begin{aligned} \frac{\mathrm{D}u}{\mathrm{D}t} - fv &= -\frac{1}{\rho_0}\frac{\partial p}{\partial x} \\ \frac{\mathrm{D}v}{\mathrm{D}t} + fu &= -\frac{1}{\rho_0}\frac{\partial p}{\partial y} \\ \frac{\mathrm{D}w}{\mathrm{D}t} &= -\frac{1}{\rho_0}\frac{\partial p}{\partial z} + b \\ \frac{\mathrm{D}b}{\mathrm{D}t} &= 0 \\ \nabla \cdot \boldsymbol{u} &= 0 \end{aligned} \tag{2.1}$$

Under the Boussinesq assumption that density fluctuations are small, the thermodynamic equation is written as equation (4) in the system above. The buoyancy is characterised by Potential Temperature, θ as $b = \frac{g\theta}{\theta_0}$. By also introducing the geopotential $\phi = \frac{p}{\rho_0}$, equations 2.1 are rewritten as

$$\begin{aligned} \frac{\mathrm{D}u}{\mathrm{D}t} - fv &= -\frac{\partial \phi}{\partial x} \\ \frac{\mathrm{D}v}{\mathrm{D}t} + fu &= -\frac{\partial \phi}{\partial y} \\ \frac{\mathrm{D}w}{\mathrm{D}t} &= -\frac{\partial \phi}{\partial z} + \frac{g\theta}{\theta_0} \\ \frac{\mathrm{D}\theta}{\mathrm{D}t} &= 0 \\ \nabla \cdot \boldsymbol{u} &= 0 \end{aligned} \tag{2.2}$$

where θ_0 and g denote initial potential temperature and acceleration due to gravity respectively.
$\frac{\mathrm{D}}{\mathrm{D}t} \equiv \frac{\partial}{\partial t} + u\frac{\partial}{\partial x} + v\frac{\partial}{\partial y} + w\frac{\partial}{\partial z}, \qquad \nabla \equiv \left(\frac{\partial}{\partial x}, \frac{\partial}{\partial y}, \frac{\partial}{\partial z}\right)$

2.1.2 The Vertical Slice Model

To facilitate the study of frontogenesis a vertical slice model is introduced. In this report the vertical slice is defined as the $(x - z)$ plane. Perturbations to the leading-order fields are considered as functions of x, z and t only, whereas the leading order terms in θ and ϕ are functions of (y, z). Retaining the potential temperature gradient normal to the slice is crucial to the subsequent evolution of the front. Following the

ideas of Yamazaki, 2017 [5] we introduce,

$$\begin{aligned} \theta &= \bar{\theta}(y,z) + \theta'(x,z,t) \\ \phi &= \bar{\phi}(y,z) + \varphi(x,z,t) \end{aligned} \tag{2.3}$$

With the background fields chosen as,

$$\begin{aligned} \bar{\theta} &= -Cy + \frac{N^2\theta_0 z}{g} \\ \frac{\partial\bar{\phi}}{\partial y} &= -\frac{Cg}{\theta_0}(z - H/2) \end{aligned} \tag{2.4}$$

The Brunt-Väisälä frequency $N^2 = \frac{g}{\theta_0}\frac{\partial\theta}{\partial z}$ characterises the stratification of density in the slice and H denotes the vertical height of the domain. The constant, normal potential temperature gradient, $\frac{\partial\theta}{\partial y} = -C$.

If the hydrostatic approximation $\frac{\mathrm{D}w}{\mathrm{D}t} = 0$ is made in addition, then the third momentum equations gives,

$$\frac{\partial\bar{\phi}}{\partial z} = -\frac{Cgy}{\theta_0} + N^2 z \tag{2.5}$$

To reach the vertical slice model we substitute $\theta = \bar{\theta} + \theta'$ and $\phi = \bar{\phi} + \varphi$ with expressions 2.4 and 2.5 into equations 2.2.

$$\begin{aligned} \frac{\mathrm{D}u}{\mathrm{D}t} - fv &= -\frac{\partial}{\partial x}\left(\bar{\phi} + \varphi\right) \\ \frac{\mathrm{D}v}{\mathrm{D}t} + fu &= -\frac{\partial}{\partial y}\left(\bar{\phi} + \varphi\right) \\ 0 &= \frac{\partial}{\partial z}\left(\bar{\phi} + \varphi\right) - \frac{g}{\theta_0}\left(\bar{\theta} + \theta'\right) \\ 0 &= \frac{\partial}{\partial t}\left(\bar{\theta} + \theta'\right) + u\frac{\partial}{\partial x}\left(\bar{\theta} + \theta'\right) + v\frac{\partial}{\partial y}\left(\bar{\theta} + \theta'\right) + w\frac{\partial}{\partial z}\left(\bar{\theta} + \theta'\right) \\ 0 &= \frac{\partial u}{\partial x} + \frac{\partial v}{\partial y} + \frac{\partial w}{\partial z} \end{aligned} \tag{2.6}$$

By neglecting $\partial/\partial y$ terms in perturbation variables after rearrangement

$$\begin{aligned}
\frac{\mathrm{D}u}{\mathrm{D}t} - fv &= -\frac{\partial\varphi}{\partial x} \\
\frac{\mathrm{D}v}{\mathrm{D}t} + fu &= -\frac{\partial\varphi}{\partial y} + \frac{Cg}{\theta_0}(z - H/2) \\
0 &= \frac{\partial\varphi}{\partial z} - \frac{g\theta'}{\theta_0} \\
0 &= \frac{\partial\theta'}{\partial t} + u\frac{\partial\theta'}{\partial x} - Cv + w\frac{\partial\theta'}{\partial z} + w\frac{N^2\theta_0}{g} \\
0 &= \frac{\partial u}{\partial x} + \frac{\partial w}{\partial z}
\end{aligned} \tag{2.7}$$

Comment: $w\frac{N^2\theta_0}{g}$ **shouldn't be there !**

2.1.3 The Geostrophic Momentum Approximation

To reach the final semi-geostrophic Eady model for frontogenesis the Geostrophic Momentum approximation is made. Developed by Hoskins, 1975 [3], where further detail can be found, the following section gives a brief summary of the key arguments.

Going back to equations 2.2. We consider an expansion in the Rossby number $\epsilon = U/fL$ where U and L are horizontal velocity and length scaled respectively. Expanding the momentum equations in 2.2 in leading-order (geostrophic) and first order (ageostrophic) terms in ϵ, so that,

$$\boldsymbol{u} = \boldsymbol{u_g} + \epsilon\boldsymbol{u_a} \qquad \phi = \phi_g + \epsilon\phi_a$$

Acceleration terms are found to be $O(\epsilon)$ so that at the leading order the geostrophic balance is found to be,

$$fv_g = -\frac{\partial\phi_g}{\partial x} \qquad -fu_g = -\frac{\partial\phi_g}{\partial y} \tag{2.8}$$

Subsequent analysis as detailed in Hoskins 1975, [3] finds the prognostic equations for ageostrophic variables to be such that the momentum $\frac{\mathrm{D}u}{\mathrm{D}t}, \frac{\mathrm{D}v}{\mathrm{D}t}$ are replaced with their geostrophic counterparts $\frac{\mathrm{D}u_g}{\mathrm{D}t}, \frac{\mathrm{D}v_g}{\mathrm{D}t}$. Noting that in the vertical slice model $u_g = 0$ we

find equations 2.7 with the geostrophic momentum approximation as

$$\begin{aligned} -fv_g + \frac{\partial \varphi}{\partial x} &= 0, \\ \frac{Dv_g}{Dt} + fu - \frac{Cg}{\theta_0}(z - H/2) &= 0, \\ \frac{D\theta'}{Dt} - Cv_g &= 0, \\ \frac{\partial \varphi}{\partial z} - g\frac{\theta'}{\theta_0} &= 0, \\ \nabla \cdot \boldsymbol{u} &= 0. \end{aligned} \tag{2.9}$$

Comment: First equation is different - $-fv_g$ isn't $O(\epsilon)$??

Where, for convenience the subscript a has been dropped. With, $\frac{\mathrm{D}}{\mathrm{D}t} \equiv \frac{\partial}{\partial t} + u\frac{\partial}{\partial x} + w\frac{\partial}{\partial z}, \qquad \nabla \equiv \left(\frac{\partial}{\partial x}, \frac{\partial}{\partial z}\right)$

The corresponding energy integral is,

$$E = \iint \frac{1}{2}v_g^2 - \frac{g\theta'}{\theta_0}(z - H/2)\,\mathrm{d}x\mathrm{d}z \tag{2.10}$$

Equations 2.9 form the basis of the subsequent investigation of frontogenesis in this report. They are to be solved over the domain $\Gamma = [-L, L] \times [0, H]$, with the periodic boundary conditions in x and the rigid-lid boundary condition $w = 0$ on $z = 0, H$. The baroclinic instability introduced from Cullen 2006 [2] in the form of a perturbation to θ',

$$\theta' = \frac{N^2\theta_0 z}{g} + B\sin\left(\pi\left(x/L + z/H\right)\right) \tag{2.11}$$

- **Key Scalings** It is worth noting that Eady's original model for baroclinic instability was developed under a quasi-geostrophic model, where $\epsilon = Fr \ll 1$ in contrastsemi-geostrophic theory the assumes, $\epsilon \ll 1$ with $\epsilon < Fr$.

Comment: does this need including?

2.2 Transformation to Geostrophic Co-ordinates

To facilitate the implementation of the numerical scheme we will subsequently use to solve equations 2.9 a "geostrophic co-ordinate"system first introduced by Hoskins [3] in the horizontal directions (x, y). The geostrophic co-ordinates describe the position of particles had they evolved under their geostrophic velocity. The transformation was later developed by Cullen [2] to include a transformation in terms of θ' in the

vertical direction.

$$X = x + \frac{v_g}{f}, \qquad Z = \frac{g\theta'}{f^2\theta_0} \tag{2.12}$$

By defining

$$P = \frac{1}{2}x^2 + \frac{1}{f^2}\varphi \tag{2.13}$$

It is clear that,

$$\nabla P = \left(x + \frac{1}{f^2}\frac{\partial\varphi}{\partial x}, \frac{1}{f^2}\frac{\partial\theta'}{\partial z}\right) \quad = \left(x + \frac{v_g}{f}, \frac{g\theta'}{f^2\theta_0}\right)$$

So that upon substitution from the first and fourth equations in 2.9 we find,

$$\nabla P = (X, Z) \tag{2.14}$$

By noting that,

$$\frac{\mathrm{D}X}{\mathrm{D}t} = \frac{\mathrm{D}x}{\mathrm{D}t} + \frac{1}{f}\frac{\mathrm{D}v_g}{\mathrm{D}t} = u + \frac{1}{f}\frac{\mathrm{D}v_g}{\mathrm{D}t}, \qquad \frac{\mathrm{D}Z}{\mathrm{D}t} = \frac{g}{f^2\theta_0}\frac{\mathrm{D}\theta'}{\mathrm{D}t}$$

the momentum equations from 2.9 are transformed into geostrophic co-ordinates as

$$\frac{\mathrm{D}X}{\mathrm{D}t} - \frac{Cg}{f\theta_0}(z - H/2) = 0, \qquad \frac{\mathrm{D}Z}{\mathrm{D}t} - \frac{Cg}{f\theta_0}(X - x) = 0, \tag{2.15}$$

It is also shown in [2] that the continuity equation holds in geostrophic co-ordinates. with $\boldsymbol{U} = \frac{Cg}{f\theta_0}(X - x, z - H/2)$ Putting together equations 2.13, 2.14, 2.15 the Eady Model in geostrophic co-ordinates is

$$\begin{aligned} \frac{\mathrm{D}X}{\mathrm{D}t} - \frac{Cg}{f\theta_0}(z - H/2) &= 0 \\ \frac{\mathrm{D}Z}{\mathrm{D}t} - \frac{Cg}{f\theta_0}(X - x) &= 0, \\ P = \frac{1}{2}x^2 + \frac{1}{f^2}\varphi, & \\ \nabla P = (X, Z) & \\ \nabla \cdot \boldsymbol{U} = 0 & \end{aligned} \tag{2.16}$$

The corresponding energy integral is,

$$E = f^2 \iint \frac{1}{2}(X - x)^2 - Z(z - H/2)\,\mathrm{d}x\mathrm{d}z \tag{2.17}$$

It is shown by Cullen [2] that the system of equations above can be recast as an optimal transport problem satisfying energy minimisation with a quadratic cost, **Comment: show that the energy minimisation is equaivalent to the equa-**

tion below

$$E = f^2 \iint \frac{1}{2} \left((X - x)^2 + (Z - z)^2 \right) \mathrm{d}x\mathrm{d}z \tag{2.18}$$

Chapter 3

Formulation as an Optimal Transport Problem

The Damped Newton algorithm developed by Mérigot et al. [6] solves a semi-discrete Monge-Ampère type optimal transport problem. It's efficiency in exploiting the properties of sparse matrices and linear convergence [6] make it practical for implementation in the solution for equations 2.16. Further detail describing the application of the algorithm in the solution to the Eady Model is given in chapter 4. In this chapter an overview of semi-discrete optimal transport is given using definitions given in [7, 6] as well as a comparison to the energy minimisation to which it is applied. A rigorous proof of the formulation of 2.9 as a Monge-Ampère type optimal transport problem is given in Cullen, 2006 [2].

3.1 Semi-discrete Optimal Transport

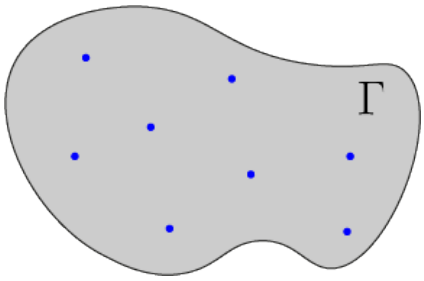

Figure 3.1: A discrete (target) set $Y \subseteq \mathbb{R}^2$ represented by blue points in a compact domain (source) $\Gamma \subseteq \mathbb{R}^2$

Optimal transport problems describe the problem of finding a map between two sets, each with an associated density, in such a way that the "cost" associated with the mapping is minimised. In semi-discrete optimal transport the target set is a finite set.

In Kitagawa et al. [7] a wonderful analogy with travel distance to bakeries in a city is made. The example considers a population in the city and a finite set of locations of bakeries in the city. It is assumed that the population is uniformly distributed in the city. The optimal transport problem finds a partition of the city such that every point in a region of the partion is closest to the bakery at the centre of that region. In this analogy the cost being minimised is the travel distance to the bakery $c(\boldsymbol{x}, \boldsymbol{y}_i) = \|\boldsymbol{x} - \boldsymbol{y}_i\|^2$. This is illustrated in figure 3.2 below

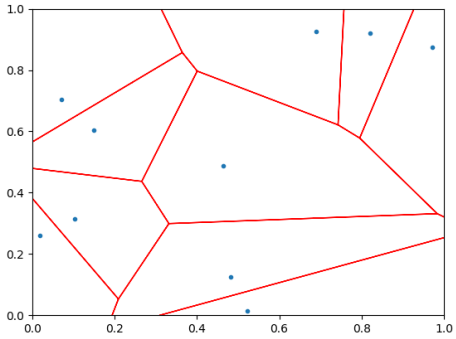

Figure 3.2: The image showing how a city would be divided into areas based on minimising distance to the local bakeries denoted by blue points

To put this into a more rigorous mathematical setting, given a domain $\Gamma \subseteq \mathbb{R}^2$ and discrete set of N points $Y = \{\boldsymbol{y}_i, \quad 1 \leq i \leq N\} \subset \mathbb{R}^2$,

Source measure $\mu(A) = \int_A \rho(x)dx$, $A \subseteq \Gamma$ with ρ a probability density on Γ
The **Target measure** $\nu = \sum_{1 \leq i \leq N} \nu_i \delta_{y_i}$, with finite support on $\mathbb{R}^2$, where $\nu_i \in \mathbb{R}$ and δ_{y_i} is the delta function centred at the point $\boldsymbol{y}_i$

The partition of the city is described mathematically by **Voronoi Cells**
$\text{Vor}_y := \{x \in \Gamma \text{ st } \forall z \in Y \; c(x, y) \leq c(x, z)\}$

Following [7] we then define a **Transport map**, $T : \Gamma \to Y$ between the source measure μ and the target measure on Y, μ if $T_{\#}\mu = \nu$.

The **Pushforward** of a measure μ by a map $T : \Gamma \to Y$ is $T_{\#}\mu = \sum_{\boldsymbol{y}_i \in Y} \mu\left(T^{-1}(\boldsymbol{y}_i)\right) \delta_{\boldsymbol{y}_i}$, the sum of the measures of the set mapped to the point $\boldsymbol{y}_i$ under T
From these definitions we can see that the optimal transport map is given by,

$$T(x) = \arg\min_{y \in Y} \left(c(x, y)\right) \tag{3.1}$$

or equivalently if

$$\nu_i = \mu\left(\mathrm{Vor}_{y_i}\right) \tag{3.2}$$

Figure 3.2 above shows the Voronoi diagram for the example of bakeries in a city **Comment: not sure about this section - also a lot of it is paraphrased from the [7] paper**

3.2 Laguerre Cells and the Inclusion of weights

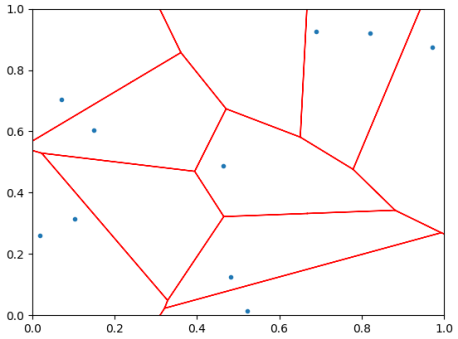

Figure 3.3: Given a uniform source and target density the Laguerre diagram produced by finding weights using damped newton algorithm for optimal transport

Considering again the example of bakeries in the city, looking at figure 3.2 it is clear that if the population density across city is uniform the distribution of customers to each bakery is certainly not. For example, the Voronoi cell at the centre of the diagram is much larger in area than those in the top right of the diagram. This raises the problem of finding a way to create a partion so that each cell has the same area. This is done by introducing an additional "weight "argument to the cost. We denote the weights by $\psi_i = \psi\left(\boldsymbol{y}_i\right)$. In the case of the bakeries the weights might represent the price of bread at a specific bakery. For example in figure 3.2 if the bakery at the centre charged more for bread the population living on the outskirts of the cell would be more incentivised to travel further for cheaper bread.

The cells are now called **Laguerre Cells**, defined as
$\mathrm{Lag}_{y_i}(\psi) := \{x \in K \text{ st } \forall y_j \in Y \; c(x,y) + \psi(y_i) \leq c(x,z) + \psi(y_j)\}$

In this case, the optimal transport map is given by
$T_\psi : x \to \mathrm{argmin}_i \|x - y_i\|^2 + \psi_i$, where $\psi_i = \psi(y_i)$ is a family of weights on Y [6].

The problem is then finding the weights ψ_i associated to the points y_i such that $G_i(\psi) := \mu(\text{Lag}_{y_i}(\psi)) = \nu_i$. The Damped Newton's Algorithm from Mérigot, Meyron and Thibert (2017) [6] finds such ψ_i.

Supposing that both the source density and target density are uniform, the Laguerre cells as found by the code developed in [6] are show in figure 3.3. The cells in this case are the Laguerre cells defined above, and the optimal transport map was found by [6] as

$$T(x) = \arg\min_{y \in Y} \left(c(x, y) + \psi_i(y)\right)$$

For the remainder of this report we will consider cases where both the source density and target density are uniform and the quadratic cost function

$$c(x, y) = \|x - y\|^2$$

3.3 Applying semi-discrete optimal transport to solving the semi-geostrophic equations

As shown in [2] equations 2.9 can be recast as an optimal transport problem using the transformation to geostrophic co-ordinates introduced by Hoskins [3]. In this section we outline how the damped newton algorithm is applied to equations 2.9.

The optimal transport problem considered in the frontogenesis problem is the minimisation of the energy, restated from equation 2.17

$$E = f^2 \iint \frac{1}{2}(X - x)^2 - Z\,(z - H/2)\,\mathrm{d}x\mathrm{d}z \tag{3.3}$$

as show in section 2.1.3 this is equivalent to minimising 2.18

$$E = \frac{f^2}{2} \iint \left((X - x)^2 + (Z - z)^2\right) \mathrm{d}x\mathrm{d}z \tag{3.4}$$

Considering the geostrophic co-ordinates as the target set of finite set of points for the optimal transport problem from the domain $\Gamma = [-L, L] \times [0, H]$. The Damped Newton Algorithm finds the weights such that the area of each Laguerre cell is preserved.

3.4 Extension for Periodic Boundary Conditions

As stated in Chapter 2 in the model for frontogenesis boundary conditions consider periodicity in x. This must be accounted for in the implementation of the Damped Newton Algorithm.

This inclusion of periodic boundary conditions means that Laguerre cells may cover areas over the right and left boundaries. This means that the Laguerre edges must be continuous across the boundaries if copies of the Laguerre diagram were placed on each boundary. As well as all the Laguerre cells must have the same mass. This is illustrated in the Laguerre diagram in figure **Comment: insert periodic Laguerre diagram and explain**
A detailed explanation of how this was implemented for solving the semi-geostrophic equations is included in section 4.3.

Comment: include the definition of mass of a cell and a better written description of the partion given by a laguerre diagram (tesselation/zero measure sets)

Chapter 4

A Numerical Solution to the Eady Model for Frontogenesis

In this section the numerical implementation including the use of the Damped Newton Algroithm developed by [6] is explained in detail. Restating the problem, we are solving the semi-geostrophic equations 2.9 over the domain $\Gamma := [-L, L] \times [0, H]$.

$$\begin{aligned} -fv_g + \frac{\partial \varphi}{\partial x} &= 0, \\ \frac{Dv_g}{Dt} + fu - \frac{Cg}{\theta_0}(z - H/2) &= 0, \\ \frac{D\theta'}{Dt} - Cv_g &= 0, \\ \frac{\partial \varphi}{\partial z} - g\frac{\theta'}{\theta_0} &= 0, \\ \nabla \cdot \boldsymbol{u} &= 0. \end{aligned}$$

With boundary conditions:

- Rigid lid condition $w = 0$ on $z = 0, H$
- Periodic boundary conditions in x

Together with a baroclinic instability described by 2.11 as

$$\theta' = \frac{N^2 \theta_0 z}{g} + B \sin\left(\pi \left(x/L + z/H\right)\right) \tag{4.1}$$

The steps involved in solving the Eady Model for frontogenesis described above are detailed below,

Step 1 Initialise a set of physical points in space

Step 2 Transform physical points to Geostrophic space using the co-ordinate transformation given in 2.1.3

Step 3 Given the points in geostrophic space the weights which define the Laguerre

cells in the physical domain are calculated using the Damped Newton Algorithm.

Step 4 The equations are now time stepped from the transformed momentum equations 2.16

$$\frac{\mathrm{D}X_n}{\mathrm{D}t} - \frac{Cg}{f\theta_0}(\tilde{z}_n - H/2) = 0$$
$$\frac{\mathrm{D}Z_n}{\mathrm{D}t} - \frac{Cg}{f\theta_0}(X_n - \tilde{x}_n) = 0$$

Where X_n, Z_n represent the geostrophic points at the current time step, and $\tilde{x}_n, \tilde{z}_n$ represent the centroids of the Laguerre cells. In this project both a Forward-Euler scheme and Heun's method have been used for time-stepping.

Step 5 The geostrophic points are now replaced with X_{n+1}, Z_{n+1} and steps 3 and 4 are repeated until the final time is reached.

Comment: include pseudocode overview??

4.1 Initialisation of Points in Geostrophic Space

Given a finite set of equidistant points in the physical domain Γ, the points are transformed to geostrophic space using

$$X = x + \frac{v_g}{f}, \qquad Z = \frac{g\theta'}{f^2\theta_0} \tag{4.2}$$

This requires the form of θ' given by 2.11 from this v_g can be deduced using the following equations from 2.9,

$$\begin{aligned} \frac{\partial\varphi}{\partial z} - \frac{g\theta'}{\theta_0} &= 0 \\ \frac{\partial\varphi}{\partial x} - fv_g &= 0 \end{aligned} \tag{4.3}$$

using the boundary condition $\int_0^H \varphi(x,z)\,\mathrm{d}z = 0$ Integrating the first equation in z,

$$\frac{\partial\varphi}{\partial z} = \frac{g\theta'}{\theta_0} = N_0^2 z + \frac{Bg}{\theta_0}\sin\left(\pi\left(\frac{x}{L} + \frac{z}{H}\right)\right)$$
$$\varphi = \frac{N_0^2 z^2}{2} - \frac{BgH}{\theta_0\pi}\cos\left(\pi\left(\frac{x}{L} + \frac{z}{H}\right)\right) + F(x)$$

Applying the boundary condition to determine $F(x)$,

$$\int_0^H \varphi\,\mathrm{d}z = \left[\frac{N_0^2 z^3}{6} - \text{`}\frac{BgH^2}{\theta_0\pi^2}\sin\left(\pi\left(\frac{x}{L} + \frac{z}{H}\right)\right) + F(x)z\right]_0^H = 0$$

Using $\sin\left(\frac{\pi x}{L}+\pi\right) = -\sin\left(\frac{\pi x}{L}\right)$,

$$0 = \frac{N_0^2 H^3}{6} - \frac{BgH^2}{\theta_0 \pi^2}\sin\left(\frac{\pi x}{L}+\pi\right) + \frac{BgH^2}{\theta_0\pi^2}\sin\left(\frac{\pi x}{L}\right) + F(x)H$$
$$0 = \frac{N_0^2 H^3}{6} + \frac{2BgH^2}{\theta_0 \pi^2}\sin\left(\frac{\pi x}{L}\right) + F(x)H$$

This gives $F(x)$ as,

$$F(x) = -\frac{N_0^2 H^2}{6} - \frac{2BgH^2}{\theta_0\pi^2}\sin\left(\frac{\pi x}{L}\right)$$

and consequently φ as,

$$\varphi(x,z) = \frac{N_0^2 z^2}{2} - \frac{BgH}{\theta_0\pi}\cos\left(\pi\left(\frac{x}{L}+\frac{z}{H}\right)\right) - \frac{N_0^2H^2}{6} - \frac{2BgH}{\theta_0\pi^2}\sin\left(\frac{\pi x}{L}\right) \tag{4.4}$$

Using the second of equations 4.3 v_g is found as,

$$v_g = \frac{BgH}{f\theta_0 L}\cos\left(\pi\left(\frac{x}{L}+\frac{z}{H}\right)\right) - \frac{2BgH}{f\theta_0\pi}\sin\left(\frac{\pi x}{L}\right) \tag{4.5}$$

Together with θ' given by 2.11 this expression for v_g can be used to determine X and Z in geostrophic co-ordinates through the transform 4.2. **Comment: Image of transformed points??**

4.2 Choice of Initial Weights

The Laguerre diagram of this set of points shown in figure **Comment: insert image showing geostrophic points + reference to image**
with zero weights would define Laguerre cells exterior to Γ. These cells will have zero "mass "in the domain Γ. Physical intuition tells us that given the rigid lid and periodic boundary conditions points would physically not be able to leave the domain. However, thinking of fluid particles as the centroids of Laguerre cells, a cell outside the domain would represent a fluid particle on the exterior of the domain. This also poses a problem with respect to the implementation of the Damped Newton Algorithm, as emphasised in [6], as it requires $\mu\left(\mathrm{Lag}_{y_i}(\psi)\right)$ to be a monotonic function of $\psi = (\psi(y_1), ..., \psi(y_N))$ where N is the number of points initialised in Γ. According to [6] this occurs near points where the Laguerre cells contain positive mass over Γ.

Fortunately, a solution is provided in [6]. Proposition 25 in the paper proves that if

the initial weights are given by,

$$\psi_i^0 = d\left(\boldsymbol{Y}_i, \Gamma\right)^2$$

where $\boldsymbol{Y}_i = (X_i, Z_i)$ are the points in geostrophic space. Since the domain is rectangular vertical distance from the point to the upper or lower boundary of the domain. The boundaries, given by $z = 0$ and $z = H$ are also perturbed to guarantee strict positivity of the mass of the Laguerre cells,

$$\psi_i^0 = \begin{cases} \left(Z_i - 0.9H\right)^2, & Z_i > 0.9H \\ \left(Z_i - 0.1H\right)^2, & Z_i < 0.1H \end{cases}$$

Comment: Address disparity with paper '-' sign - convention used in paper for finding laguerre cells different to code?

The Damped newton algorithm is initialised with the the geostrophic points and weights given by 4.2. The algorithm outputs weights that give Laguerre cells with equal mass over the periodic domain.

4.3 Time Stepping

4.3.1 Forward-Euler Scheme

The numerical solution to equations 2.9 developed follows a Lagrangian framework, thus it is justified to treat the material derivative $\frac{\mathrm{D}}{\mathrm{D}t}$ as the usual $\frac{\mathrm{d}}{\mathrm{d}t}$, in this sense we will develop prognostic scheme using the equations,

$$\begin{aligned} \frac{\mathrm{d}X}{\mathrm{d}t} - \frac{Cg}{f\theta_0}\left(\tilde{z} - H/2\right) = 0 \\ \frac{\mathrm{d}Z}{\mathrm{d}t} - \frac{Cg}{f\theta_0}\left(X - \tilde{x}\right) = 0 \end{aligned}$$

Applying a Forward-Euler scheme for time-stepping given by,

$$\begin{aligned} t_i^{n+1} &= t_i^n + h \\ Z_i^{n+1} &= Z_i^n + \frac{hCg}{f\theta_0}\left(X_i^n - \tilde{x}_i^n\right) \\ X_i^{n+1} &= X_i^n + \frac{hCg}{f\theta_0}\left(\tilde{z}_i^n - H/2\right) \end{aligned} \tag{4.6}$$

where $\tilde{x}_i^n, \tilde{z}_i^n$ represent the centroids of the Laguerre cells given by X_i^n, Z_i^n and corresponding weights given by the optimal transport algorithm,

$$\tilde{x}_i^n = \frac{\int_{\mathrm{Lag}_{Y_i^n}(\psi)} x \mathrm{d}x\mathrm{d}z}{\int_{\mathrm{Lag}_{Y_i^n}(\psi)} \mathrm{d}x\mathrm{d}z}, \qquad \tilde{z}_i^n = \frac{\int_{\mathrm{Lag}_{Y_i^n}(\psi)} z \mathrm{d}x\mathrm{d}z}{\int_{\mathrm{Lag}_{Y_i^n}(\psi)} \mathrm{d}x\mathrm{d}z} \tag{4.7}$$

Before the next iteration of the time-step the points X_i^{n+1}, Z_i^{n+1} are mapped back to the fundamental domain.

4.3.2 Heun's Method

Comment: include map back to fundamental domain explanation and why this isn't done for centroids

4.4 Visualising the Output

Chapter 5

Unsorted

5.1 Linear Stability Analysis

Starting from the Eady Model 2.9 restated below

$$\begin{aligned} -fv_g + \frac{\partial \varphi}{\partial x} &= 0, \\ \frac{Dv_g}{Dt} + fu - \frac{Cg}{\theta_0}(z - H/2) &= 0, \\ \frac{D\theta'}{Dt} - Cv_g &= 0, \\ \frac{\partial \varphi}{\partial z} - g\frac{\theta'}{\theta_0} &= 0, \\ \nabla \cdot \boldsymbol{u} &= 0. \end{aligned} \tag{5.1}$$

Linearise about a base state given by Hoskins [3],

$$\begin{aligned} \bar{\theta} &= \theta_0 \frac{N_0^2 \theta_0 z}{g} - Cy \\ \bar{\varphi} &= \theta_0 + \frac{N_0^2 z^2}{2} \\ \bar{v}_g &= 0 \\ \bar{U} &= \frac{Cg}{f\theta_0}(z - H/2) \\ \bar{W} &= 0 \end{aligned} \tag{5.2}$$

Introduce a perturbation and linearise about base state,
$u = \bar{U} + u'$, $w = w'$, $v_g = v_g'$, $\varphi = \bar{\varphi} + \varphi'$, $\theta' = \bar{\theta} + \theta''$
Introducing the stream function,

$$u' = \frac{\partial \psi}{\partial z}, \qquad w' = -\frac{\partial \psi}{\partial x} \tag{5.3}$$

Looking for normal modes solutions of the form,

$$q' = \hat{q}(z)\exp^{i(kx-\omega t)}$$

Equations 5.1 become,

$$-f\hat{v}_g + ik\hat{\varphi} = 0, \tag{5.4}$$

$$-i\omega\hat{v}_g + ik\bar{U}\hat{v}_g + f\frac{\mathrm{d}\hat{\psi}}{\mathrm{d}z} = 0, \tag{5.5}$$

$$-i\omega\hat{\theta} + ik\bar{U}\hat{\theta} - ik\frac{N_0^2\theta_0}{g}\hat{\psi} - C\hat{v}_g = 0, \tag{5.6}$$

$$\frac{\mathrm{d}\hat{\varphi}}{\mathrm{d}z} - g\frac{\hat{\theta}}{\theta_0} = 0, \tag{5.7}$$

First eliminating, φ, equations 5.4 and 5.7 give,

$$-f\frac{\mathrm{d}\hat{v}_g}{\mathrm{d}z} + ik\frac{\mathrm{d}\hat{\varphi}}{\mathrm{d}z} = 0, \qquad \frac{\mathrm{d}\hat{\varphi}}{\mathrm{d}z} - g\frac{\hat{\theta}}{\theta_0} = 0$$

so that,

$$\hat{\theta} = \frac{f\theta_0}{ikg}\frac{\mathrm{d}\hat{v}_g}{\mathrm{d}z} \tag{5.8}$$

Rearranging equation 5.6

$$i\left(k\bar{U} - \omega\right)\hat{\theta} - ik\frac{N_0^2\theta_0}{g}\hat{\psi} - C\hat{v}_g = 0 \tag{5.9}$$

Eliminating $\hat{\theta}$ using 5.8

$$\frac{f\theta_0}{kg}\left(k\bar{U} - \omega\right)\frac{\mathrm{d}\hat{v}_g}{\mathrm{d}z} - ik\frac{N_0^2\theta_0}{g}\hat{\psi} - C\hat{v}_g = 0$$

from equation 5.5 we have

$$i\left(k\bar{U} - \omega\right)\hat{v}_g - f\frac{\mathrm{d}\hat{\psi}}{\mathrm{d}z} = 0 \tag{5.10}$$

differentiating this expression we find

$$ik\frac{\mathrm{d}\bar{U}}{\mathrm{d}z}\hat{v}_g + i(k\bar{U} - \omega)\frac{\mathrm{d}\hat{v}_g}{\mathrm{d}z} + f\frac{\mathrm{d}^2\psi}{\mathrm{d}z^2} = 0$$

Substituting this expression with 5.10 into 5.9, noting that,

$$(k\bar{U} - \omega)\frac{\mathrm{d}\hat{v}_g}{\mathrm{d}z} = if\frac{\mathrm{d}^2\psi}{\mathrm{d}z^2} + \frac{fk}{i(k\bar{U} - \omega)}\frac{\mathrm{d}\bar{U}}{\mathrm{d}z}\frac{\mathrm{d}\hat{\psi}}{\mathrm{d}z}$$

$$\frac{f\theta_0}{kg}\left(if\frac{\mathrm{d}^2\psi}{\mathrm{d}z^2}+\frac{fk}{i(k\bar{U}-\omega)}\frac{\mathrm{d}\bar{U}}{\mathrm{d}z}\frac{\mathrm{d}\hat{\psi}}{\mathrm{d}z}\right)-\frac{ikN_0^2\theta_0\hat{\psi}}{g}+\frac{Cf}{i(k\bar{U}-\omega)}\frac{\mathrm{d}\psi}{\mathrm{d}z}=0$$

Rearranging gives,

$$-\frac{f^2\theta_0}{kg}(k\bar{U}-\omega)\frac{\mathrm{d}^2\psi}{\mathrm{d}z^2}+\left(Cf+\frac{f^2\theta_0}{g}\frac{\mathrm{d}\bar{U}}{\mathrm{d}z}\right)\frac{\mathrm{d}\hat{\psi}}{\mathrm{d}z}+\frac{kN_0^2\theta_0}{g}(k\bar{U}-\omega)\hat{\psi}=0$$

$$-f^2\theta_0(k\bar{U}-\omega)\frac{\mathrm{d}^2\psi}{\mathrm{d}z^2}+2Cfkg\frac{\mathrm{d}\hat{\psi}}{\mathrm{d}z}+k^2N_0^2\theta_0(k\bar{U}-\omega)\hat{\psi}=0$$

We reformulate this as a matrix eigenvalue problem for ω

$$-f^2\theta_0\bar{U}\frac{\mathrm{d}^2\psi}{\mathrm{d}z^2}+2Cfkg\frac{\mathrm{d}\hat{\psi}}{\mathrm{d}z}+k^2N_0^2\theta_0\bar{U}\hat{\psi}=\omega\left(k^2N_0^2\theta_0\hat{\psi}-f^2\theta_0\frac{\mathrm{d}^2\psi}{\mathrm{d}z^2}\right) \tag{5.11}$$

Introducing a second order finite difference scheme for ψ

$$\frac{\mathrm{d}^2\hat{\psi}}{\mathrm{d}z^2}=\frac{\psi_{i-1}-2\psi_i+\psi_{i+1}}{h^2}$$
$$\frac{\mathrm{d}\hat{\psi}}{\mathrm{d}z}=\frac{\psi_{i-1}-\psi_{i+1}}{2h}$$

Equation 5.11 becomes

$$\begin{aligned}-f^2\theta_0\bar{U}_i\left(\frac{\psi_{i-1}-2\psi_i+\psi_{i+1}}{h^2}\right)+2Cfkg\left(\frac{\psi_{i-1}-f\psi_{i+1}}{2h}\right)+k^3N_0^2\theta_0\bar{U}_i\psi_i=\\ \omega\left(k^2N_0^2\theta_0\psi_i-f^2\theta_0\left(\frac{\psi_{i-1}-2\psi_i+\psi_{i+1}}{h^2}\right)\right)\end{aligned} \tag{5.12}$$

Discretising the interval $[0,H]$ into N points with step size h we can recast this as an eigenvalue problem,

$$A\boldsymbol{\psi}=\omega B\boldsymbol{\psi}$$

to find eigenvalues ω with corresponding eigenvectors $\boldsymbol{\psi}=(\psi_1,...,\psi_{N-2})$. Since the boundary condition gives $\psi=0$ on $z=0,H$, $\psi_0=\psi_N=0$ so these are omitted from the $\hat{\phi}$ vector but considered in the finite difference schemes for ψ_1 and ψ_{N-1} The coefficients matrix A are given by

$$\begin{aligned}\psi_{i-1}:&\quad -\frac{-f^2\theta_0k\bar{U}_i}{h^2}-\frac{Cfkg}{h}\\ \psi_i:&\quad \frac{2f^2\theta_0k\bar{U}_i}{h^2}+k^3N_0^2\theta_0\bar{U}_i\\ \psi_{i+1}:&\quad \frac{-f^2\theta_0k\bar{U}_i}{h^2}+\frac{Cfkg}{h}\end{aligned} \tag{5.13}$$

$i : 1 \to N-2$ with $\psi_0 = \psi_N$. The coefficients of matrix B are given by,

$$\begin{aligned} \psi_{i-1} : &\quad -\frac{f^2\theta_0}{h^2} \\ \psi_i : &\quad k^2 N_0^2 \theta_0 + \frac{2f^2\theta_0}{h^2} \\ \psi_{i+1} : &\quad -\frac{f^2\theta_0}{h^2} \end{aligned}$$

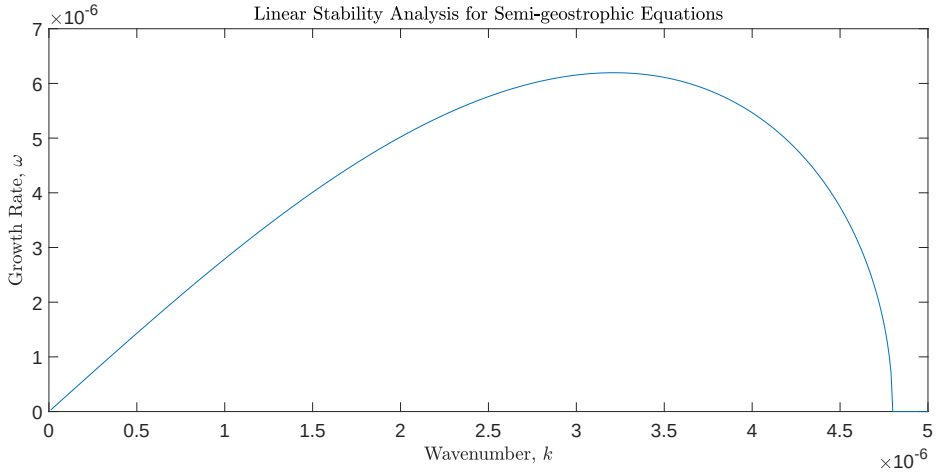

Figure 5.1: Plot showing growth rate, ω against wavenumber k for the Eady model of the semi-geostrophic equations

5.2 Calculation of Moments applying periodic boundary conditions

Chapter 6

Numerical Simulations and Results

6.1 Evolution of Average Kinetic Energy

Chapter 7

Conclusion

Appendix A

First Appendix

Bibliography

[1] A. Eliassen. On the vertical circulation in the frontal zones. *Geofysiske Publikasjoner*, 4(4):147–160, 1962.

[2] Michael J P Cullen. *A Mathematical Theory of Large-scale Atmosphere/ocean Flow*. Imperial College Press, jan 2006.

[3] Brian J. Hoskins. The Geostrophic Momentum Approximation and the Semi-Geostrophic Equations. *Journal of the Atmospheric Sciences*, 32(2):233–242, 1975.

[4] B. J. Hoskins and F. P. Bretherton. Atmospheric Frontogenesis Models: Mathematical Formulation and Solution. *Journal of the Atmospheric Sciences*, 29(1):11–37, jan 1972.

[5] Hiroe Yamazaki, Jemma Shipton, Michael J.P. Cullen, Lawrence Mitchell, and Colin J. Cotter. Vertical slice modelling of nonlinear Eady waves using a compatible finite element method. *Journal of Computational Physics*, 343:130–149, aug 2017.

[6] Quentin Mérigot, Jocelyn Meyron, and Boris Thibert. An algorithm for optimal transport between a simplex soup and a point cloud. 2017.

[7] Jun Kitagawa, Quentin Mérigot, and Boris Thibert. Convergence of a Newton algorithm for semi-discrete optimal transport. 2016.